



Instrument Science Report WFC3 2000-05

# WFC3 Detector Characterization

## Report # 1: CCD44 Radiation Test Results

---

Laura Cawley, Christopher Hanley  
October 30, 2000

---

### ABSTRACT

*We present the results of charge transfer efficiency (CTE) measurements of a Marconi CCD. The device is a model CCD44, similar to the WFC3 flight device, a CCD43. The device is coated to improve UV response. We present the results before and after the device has been exposed to one year's equivalent on-orbit radiation. CTE is measured with three techniques:  $^{55}\text{Fe}$ , Extended Pixel Edge Response (EPER) and First Pixel Response (FPR) (post-rad only). All data were collected at the Detector Characterization Lab (DCL) at Goddard Space Flight Center. Visit <http://dcl.gsfc.nasa.gov/> for more information.*

---

### 1.) Description of CCD44s

The WFC3 engineering CCDs are standard scientific grade devices, model number CCD44-82, manufactured by Marconi of Chelmsford, UK. CCD44s are backside illuminated with a 2048 x 4102, 15  $\mu\text{m}$  square, pixel format. The device can be operated in either a full-frame mode, or in frame-transfer mode. There are 2049 rows in the image area and 2053 rows in the frame store section. The devices have 53 serial physical prescan pixels in the serial register. The serial and parallel overscan regions are readout dependent. For these measurements the parallel overscan was 98 pixels and the serial overscan was 73 pixels (23 for pre-rad CCD44V1 data). More information on the CCD44 model can be found at the Marconi website (<http://www.marconitech.com/>).

The results presented here are from a UV coated CCD44-82, hereafter called CCD44UV1. Its serial number is SN 8462-9-2. Data have been acquired from another engineering device, serial number SN 8462-6-1, referred to as CCD44V1. The coating on CCD44V1 is not UV optimized. The results for CCD44V1 will be reported elsewhere, although we note that the CTE values are consistent with those for the CCD44UV1.

### 2.) Charge Transfer, CTE, CTI and Radiation Damage

Charge transfer is characterized by CTE (charge transfer efficiency), the fraction of charge successfully transferred from one pixel to the next. Alternatively, it is characterized by CTI (charge transfer inefficiency), which is simply (1-CTE). In a perfect device, there would be no charge loss and CTE would equal 1. Actual devices experience minor loss due to traps inherent in the bulk silicon material of the CCD. A good CTE value differs from unity by few parts in  $10^6$  and a typical measurement for a scientific grade device is at least 0.999995. The number of traps increases over the lifetime of a spaceborne CCD due to radiation damage. The charge

transfer efficiency decreases, affecting the performance of the CCD. The goal of the radiation tests is to simulate the damage that will be seen by WFC3 CCDs in order to evaluate the performance of the potential flight devices and to develop methods of mitigating the effects.

### 3.) Irradiation

The devices were taken to the Crocker Nuclear Laboratory at the University of California at Davis for irradiation. They were exposed to 63 MeV protons to simulate exposures equivalent to that seen in the HST orbit. The one-year equivalent dose equals  $1.0E09$  protons/cm<sup>2</sup>. CCD44V1 was irradiated to the one-year level on February 23, 2000. CCD44UV1 was irradiated to the same level on May 4, 2000. The irradiation occurred at room temperature. The devices were not operated during irradiation.

### 4.) Cosmetics

The CCD44UV1 detector has 15 bad columns that were eliminated from the measurements either by masking (<sup>55</sup>Fe) or by median filtering (EPER and FPR). These columns are listed in Table 1. The device also has several blemishes (dark or light patches) and non-uniformity (~10 %) across the surface. It appears, by inspection, that the device was not completely polished, which is not unusual for an engineering device. A flatfield image is shown in Figure 1. It illustrates the cosmetic properties of this device. The image is split since it was read out through two amplifiers. Amplifier A is located at the bottom left corner and Amplifier B is located at the bottom right corner. There are three dark regions in the image that should be noted. The 53 columns on the left and right edges are the serial prescan for Amp A and Amp B, respectively. The region in the middle is the serial overscan for Amp A and Amp B, 73 columns each. The region at the top of the image is 98 rows of parallel overscan.

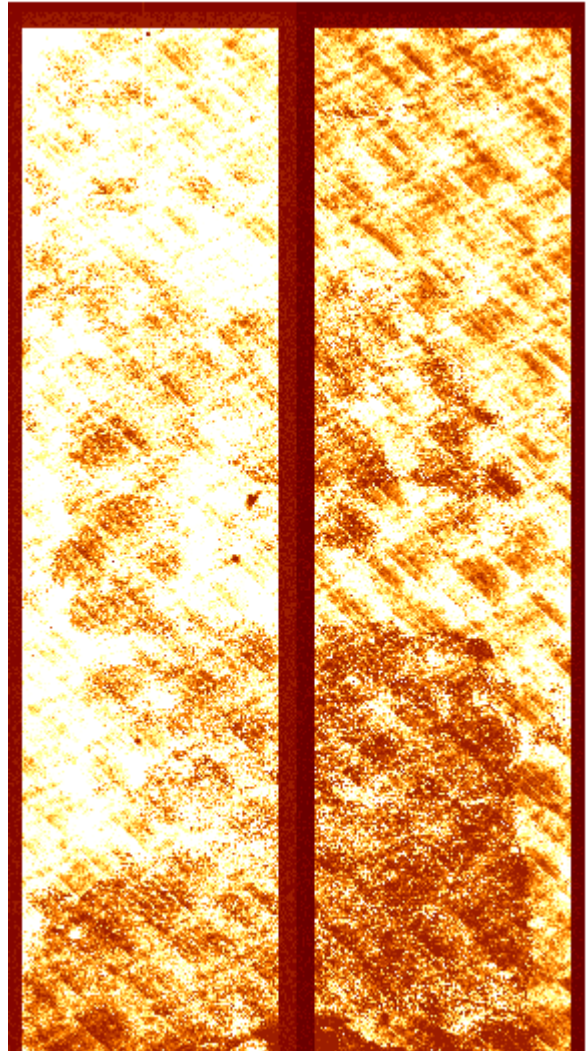


Figure 1.

**Table 1. CCD44UV1: Bad Columns**

| Bad Columns (counting from amplifier) |       |
|---------------------------------------|-------|
| Amp A                                 | Amp B |
| 12                                    | 1     |
| 537-541                               | 911   |
| 695                                   |       |
| 706                                   |       |
| 716-718                               |       |
| 724                                   |       |
| 749                                   |       |

### 5.) CTE-<sup>55</sup>Fe

The <sup>55</sup>Fe method is the most commonly used method for measuring CTE. An <sup>55</sup>Fe source emits X-ray photons at an energy of 5.89 keV, which create packets of charge in the silicon of the CCD. The charge packets have a well known size of 1614 electrons. By examining these packets at different regions of the detector, the charge loss across the detector can be determined. <sup>55</sup>Fe measurements are also a quick and convenient method of determining the gain of the CCD and camera system.

The <sup>55</sup>Fe measurements shown here are made using X-ray event selection. In this method the CCD is used as a photon counting detector to record each interaction of an X-ray photon in the CCD. This is done to deal with the actual distribution in the size of the charge packets, the fact that packets are not always contained within one pixel and to isolate the 5.89 keV line from other lines emitted from the source, as well as from cosmic rays and cosmetic defects.

Ideally each photon would deposit precisely 1614 electrons within the CCD. In reality of course, it is a distribution with a mean of 1614. Ideally, each photon and the subsequent charge packet would be isolated within one pixel. In reality, the charge is often split into two or more pixels because of diffusion. Event selection is used to isolate the 5.89 keV line and create as narrow a peak as possible so that it can be used most effectively to measure CTE. See WFC3 TIR 2000-02, "X-ray Data Analysis-Event Selection".

The data reduction for this method proceeds as follows. The data are first baseline (bias) corrected with a row-by-row sigma clipped average of the serial overscan region. All files are then combined, pixel-by-pixel, excluding events, to create a meanframe. The meanframe is subtracted from each file. X-ray events from each file are then selected and graded. (Event grades are determined by the distribution of charge. For a single event, all the charge is contained within one pixel, a singly-split has distributed in two pixels and a multiple event has charge distributed among three or more pixels.) Split and multiples grades are subdivided by location. The X-ray events for an entire dataset are combined. The events are selected by grade into a subset. The pha and center pixel value for each event is plotted versus position on the detector, i.e. versus column for serial CTE and versus row for parallel CTE. This is also known as a stacking plot. This is done for both the pha and center pixel event values; the pha event value is a combination of the signal in the central pixel plus the signal in the split. To isolate parallel CTE from serial CTE, the events are taken from positions near the output amplifier, i.e. the first 200 columns for parallel CTE and the first 400 rows for serial CTE. The results are shown in Table 2.

To measure CTE we perform a fit to the line seen in the stacking plot. The slope of this line divided by the intercept equals CTI. The error is calculated by taking the ratio of the error in the slope and the value of the intercept. Note: this error estimate will not include systematic errors

from frame to frame. The systematic error is monitored by taking the median values for each frame after baseline correction, since this method assumes only minor frame-to-frame variations. Frames which show a large variation are excluded.

The  $^{55}\text{Fe}$  technique gives a value for CTE at only one signal level. To determine CTE at other signal levels one needs to use EPER or FPR techniques (see below) or use X-ray photons at other energy levels (see WFC3 TIR 2000-01, “The use of low energy X-ray lines for CCD characterization”).

The readnoise is also determined in the reductions. It is taken in order to monitor the data; it should not be taken as the optimal performance value. The average result for each amp is shown in Table 3.

**Table 2.** CTE Results for CCD44UV1:  $^{55}\text{Fe}$  Measurement

|  | Parallel                                     |                 | Serial  |                 |
|--|--|-----------------|---|-----------------|
|  | CTI (per pixel)                              | CTE (per pixel) | CTI (per pixel)                               | CTE (per pixel) |
| Pre-radiation  |  |                 |   |                 |
| -80 C Amp A  | $2.66 \times 10^{-6} \pm 1.8 \times 10^{-7}$ | 0.99999734      | $1.26 \times 10^{-5} \pm 8.7 \times 10^{-7}$  | 0.99998763      |
| -80 C Amp B  | $4.01 \times 10^{-6} \pm 1.3 \times 10^{-7}$ | 0.99999599      | $1.22 \times 10^{-6} \pm 6.2 \times 10^{-7}$  | 0.99999878      |
|  |  |                 |   |                 |
| -90 C Amp A  | $2.64 \times 10^{-6} \pm 1.6 \times 10^{-7}$ | 0.99999736      | $3.3 \times 10^{-6} \pm 6.4 \times 10^{-7}$   | 0.99999670      |
| -90 C Amp B  | $3.34 \times 10^{-6} \pm 1.2 \times 10^{-7}$ | 0.99999666      | $0.76 \times 10^{-6} \pm 5.3 \times 10^{-7}$  | 0.99999924      |
|  |  |                 |   |                 |
| -100 C Amp A   | $4.2 \times 10^{-6} \pm 1.3 \times 10^{-7}$  | 0.99999584      | $3.2 \times 10^{-6} \pm 6.1 \times 10^{-7}$   | 0.99999676      |
| -100 C Amp B   | $4.15 \times 10^{-6} \pm 1.0 \times 10^{-7}$ | 0.99999585      | $0.39 \times 10^{-6} \pm 4.9 \times 10^{-7}$  | 0.99999961      |
|  |  |                 |   |                 |
| Post-radiation   |  |                 |   |                 |
| -80 C Amp A  | $5.44 \times 10^{-5} \pm 2.8 \times 10^{-6}$ | 0.99994564      | $1.53 \times 10^{-5} \pm 1.6 \times 10^{-6}$  | 0.99998474      |
| -80 C Amp B  | $5.58 \times 10^{-5} \pm 0.9 \times 10^{-6}$ | 0.99994423      | $1.06 \times 10^{-5} \pm 1.5 \times 10^{-6}$  | 0.99998939      |
|  |  |                 |   |                 |
| -90 C Amp A  | $5.31 \times 10^{-5} \pm \text{NA}$          | 0.99994699      | $1.45 \times 10^{-5} \pm 1.8 \times 10^{-6}$  | 0.99998552      |
| -90 C Amp B  | $5.00 \times 10^{-5} \pm \text{NA}$          | 0.99995041      | $0.98 \times 10^{-5} \pm 1.7 \times 10^{-6}$  | 0.99999023      |
|  |  |                 |   |                 |
| -100 C Amp A   | $3.31 \times 10^{-5} \pm 1.3 \times 10^{-6}$ | 0.99996698      | $1.19 \times 10^{-5} \pm 1.36 \times 10^{-6}$ | 0.99998918      |
| -100 C Amp B   | $2.84 \times 10^{-5} \pm 0.6 \times 10^{-6}$ | 0.99997160      | $0.99 \times 10^{-5} \pm 1.2 \times 10^{-6}$  | 0.99999009      |
| Gain Amp A=3.6 dn/e <sup>-</sup> , Amp B= 3.87 dn/e <sup>-</sup> (except post -80 and -100 where gain Amp A = 3.75 dn/e <sup>-</sup> ) |  |                 |   |                 |
| All results from 2s exposure data. Note: No single events were detected in the Amp A side data.  |  |                 |   |                 |

**Table 3.** Readnoise CCD44UV1:  $^{55}\text{Fe}$

|               | Readnoise (e <sup>-</sup> ) |                | Readnoise (e <sup>-</sup> ) |
|---------------|-----------------------------|----------------|-----------------------------|
| Pre-radiation |                             | Post-radiation |                             |
| -80 C Amp A   | 3.1                         | -80 C Amp A    | 2.3                         |
| -80 C Amp B   | 4.7                         | -80 C Amp B    | 2.2                         |
|               |                             |                |                             |
| -90 C Amp A   | 2.1                         | -90 C Amp A    | 2.2                         |
| -90 C Amp B   | 2.1                         | -90 C Amp B    | 2.2                         |
|               |                             |                |                             |
| -100 C Amp A  | 3.1                         | -100 C Amp A   | 2.2                         |
| -100 C Amp B  | 4.8                         | -100 C Amp B   | 2.1                         |

## 6.) CTE-Extended Pixel Edge Response (EPER)

The Extended Pixel Edge Response (EPER) technique involves exposing the CCD with a uniform, monochromatic source to create a flatfield. As the frame is readout, charge lost to CTE degradation will trail into the overscan, or extended, pixels. In the absence of charge loss, a

uniform edge would appear at the boundary of physical pixels and the overscan region. Instead, there is an exponential trail of charge that has been taken from pixels in the frame and re-emitted at a later time. A measurement of CTE is made by measuring the charge in the trail and comparing it to mean in the flatfield.

The details of the measurement are as follows: The frame is bias corrected using the sigma clipped average of each row in the serial prescan region (the overscan regions cannot be used since the charge trailing into the region would corrupt the average value).

The frame is then compressed along the dimension of interest, i.e. along the X-axis for serial CTE and along the Y-axis for parallel CTE. The values for each column or row are averaged using sigma clipping. This results in a one-dimensional array, with a length equal to the dimension of the X- or Y-axis. This array is graphically displayed so that regions within the frame (the plateau) can be selected for a linear fit. The trailing charge tail of the overscan region is also plotted. The trail falls to the baseline value. The regions for the baseline value, i.e after the trail has settled, are selected and fit with a line. The area between the plateau fit and the baseline fit contains the trailing charge. The area between the curves is integrated to determine the absolute value of the trailing charge. By comparing the plateau value to the trailing value, the CTE is determined. The equation for this calculation is:

$$CTE=(1-\Delta Q/QN)$$

where Q equals the plateau value,  $\Delta Q$  equals the trailing charge and N is the number of pixel transfers. The EPER results for Parallel CTI are shown in Figures 2a and 2b. The results for Serial CTI are shown in Figures 3a and 3b. These results are for Post-rad 1 year. EPER data were taken prior to irradiation, however there may have been a problem with the shutter causing variations in the signal levels. The data need further evaluation.

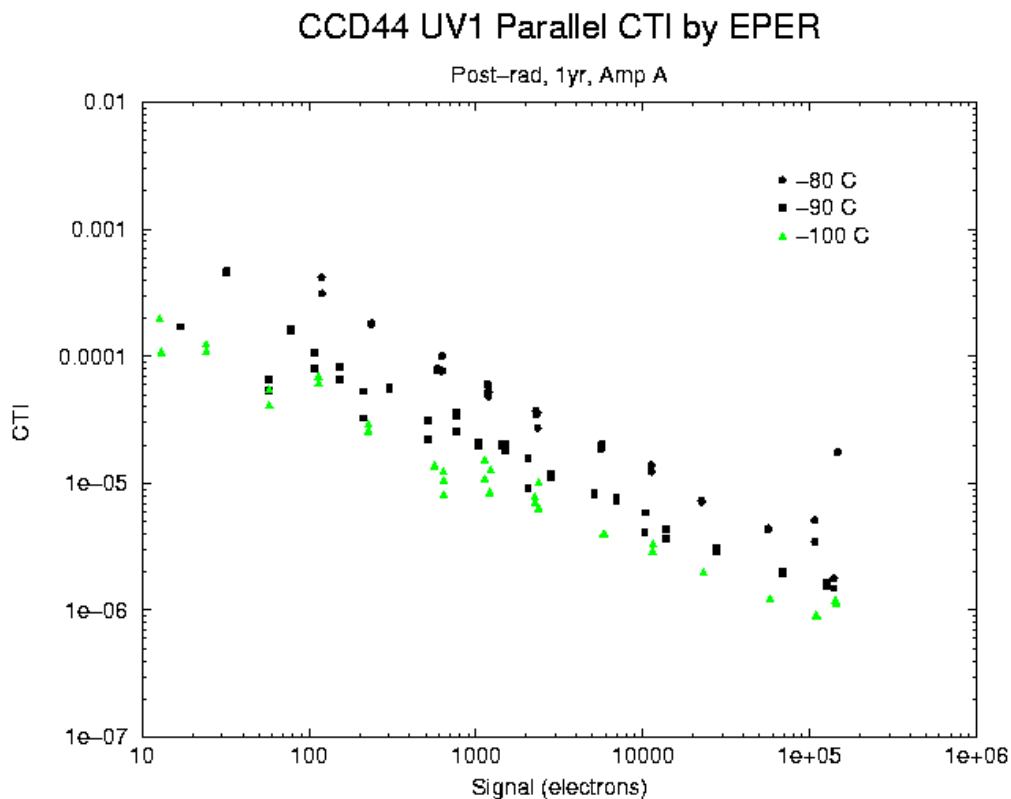
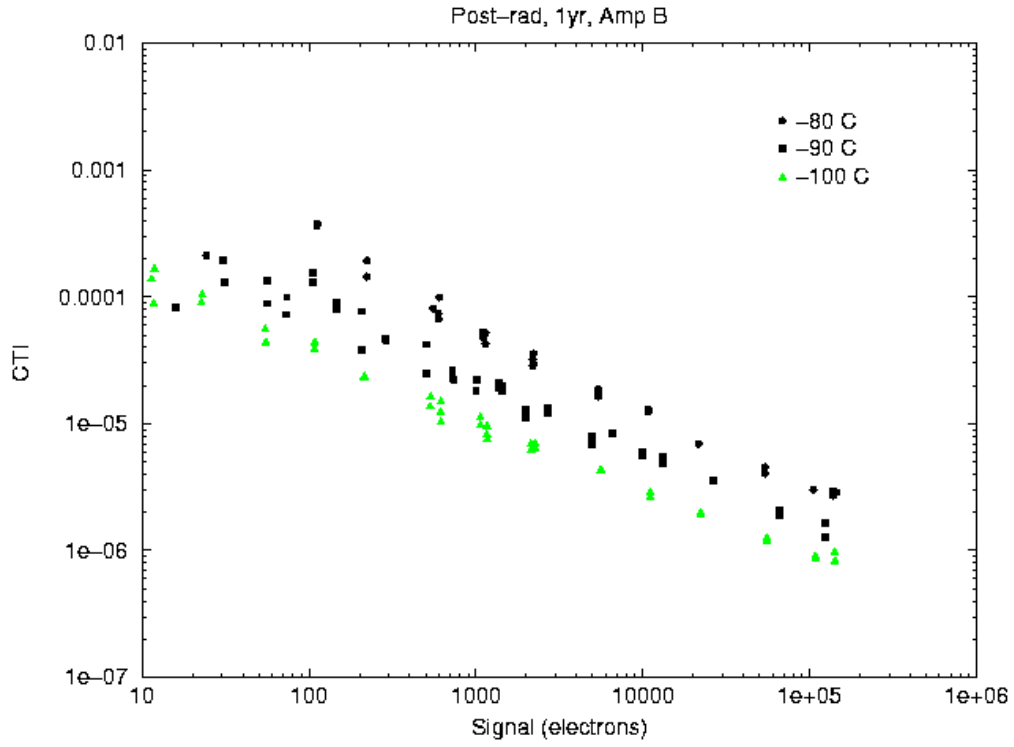


Figure 2a-Parallel CTI EPER Amp A  
CCD44 UV1 Parallel CTI by EPER



### CCD44 UV1 Serial CTI by EPER

Post-rad, 1 yr, Amp A

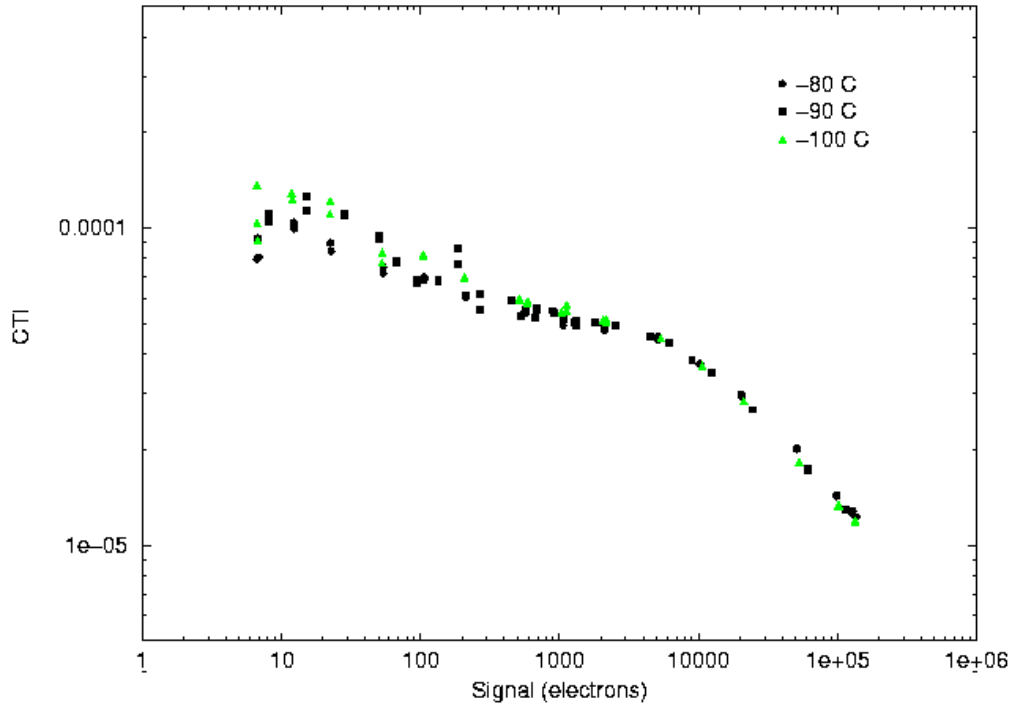


Figure 3a-Serial CTI EPER Amp A

### CCD44 UV1 Serial CTI by EPER

Post-rad, 1 yr, Amp B

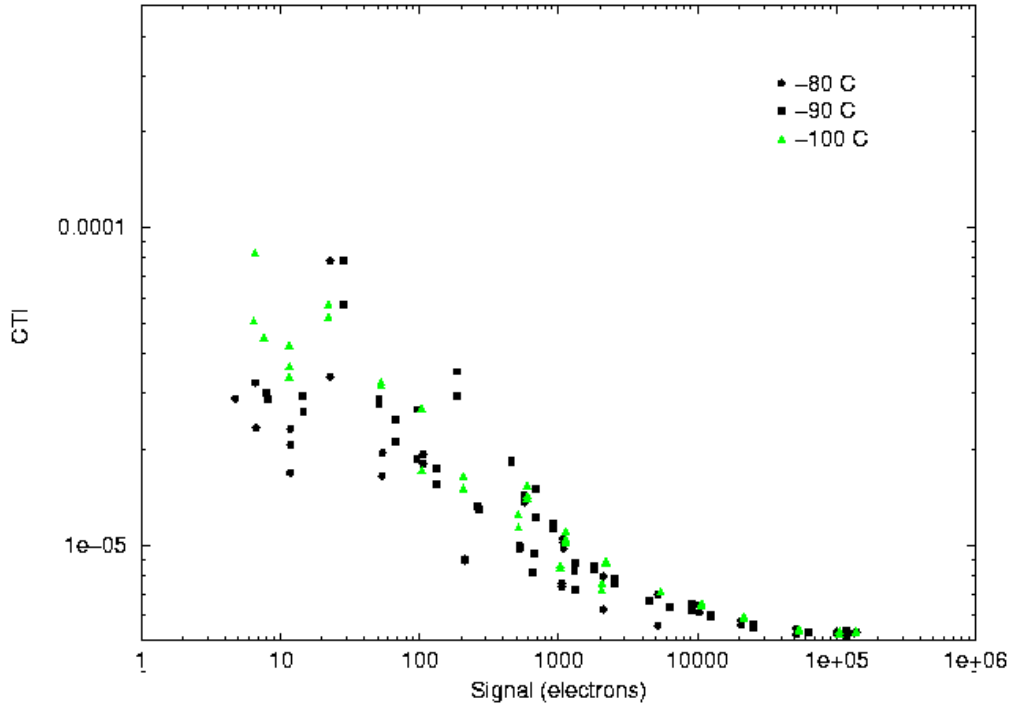


Figure 3b-Serial CTI EPER Amp B

The EPER technique is quite useful in that the illumination can be changed to create a variety of signal levels that cover the dynamic range of the CCD. CTE can be measured versus signal size from as little as 30 electrons, up to tens of thousands of electrons, or the full well capacity of the

CCD. However, it has been demonstrated that CTE measurements made using the EPER technique tend to overestimate the value of CTE. This is likely due to the filling of traps by charge from the flatfield as the detector is readout. A technique has been developed by Mike Jones and the ACS team to circumvent that bias. That technique is called First Pixel Response (FPR). See TIR ACS-99-03, “Justification and Requirements for On-board ACS FPR/EPER CTE Calibration”.

Note: There is a marked difference between the A and B amp serial CTI curves at large signal levels. In Amp B the values are approaching a constant CTI value whereas in the Amp A curve they are continuing to fall off. This may be the same effect seen in the <sup>55</sup>Fe measurements where no signal events are seen through the A amplifier; visual inspection shows that all potential single events are split to the right. It is certainly the reason for the higher CTI values for Amp A at all signal levels.

### 7.) CTE-First Pixel Response (FPR)

The FPR technique is similar to the EPER technique in that the CCD is exposed to a uniform, monochromatic source to create a flatfield. The difference in FPR is that half the frame (nearest the output amp) is clocked out, flushing the charge and creating a leading (instead of a trailing) edge. The detector is then readout normally. As the leading row (or column) of the flatfield charge is clocked through the flushed region, it loses charge to traps in that region. The difference between the charge in the first pixel of the flat (which has been depleted by trapping) and the fit of the remaining pixels is the measure of CTE. The equation is the same as for EPER, only rearranged to represent measured values:

$$CTE=1- ((Q-Q_{fp})/QN)$$

where Q is the fitted value of the flat,  $Q_{fp}$  is the signal in the first pixel and N is the number of pixel transfers. Because a leading edge is created by flushing half the detector, there is no filling of traps and the measurement is a better representation of the CTE. The CTI versus signal level from the FPR measurement is shown in Figures 4a and 4b. Clocking is currently only available for Parallel FPR measurements. A comparison of the measurements from the three techniques is shown in Figure 5.

### Conclusions

We have obtained charge transfer efficiency (CTE) measurements on a engineering grade Marconi CCD model 44-82, a device similar to the devices that will be used in the WFC3 UVIS channel. These measurements have been made before and after irradiation in order to determine CCD performance on orbit. We find that the devices have excellent CTE before irradiation and that the CTE degrades as expected after irradiation.

We find:

- The Parallel CTE is more strongly degraded by radiation damage than Serial CTE.
- CTE improves as the temperature is decreased over the range -80 to -100 C.
- EPER measurements tend to overestimate CTE as compared to the FPR and <sup>55</sup>Fe techniques.

We also found the CCD44UV1 device to have poorer serial CTE on the left (A-amp) side of the chip either due to damage in the serial register on that side or as a result of reading out through amplifier A.

### CCD44 UV1 Parallel CTI by FPR

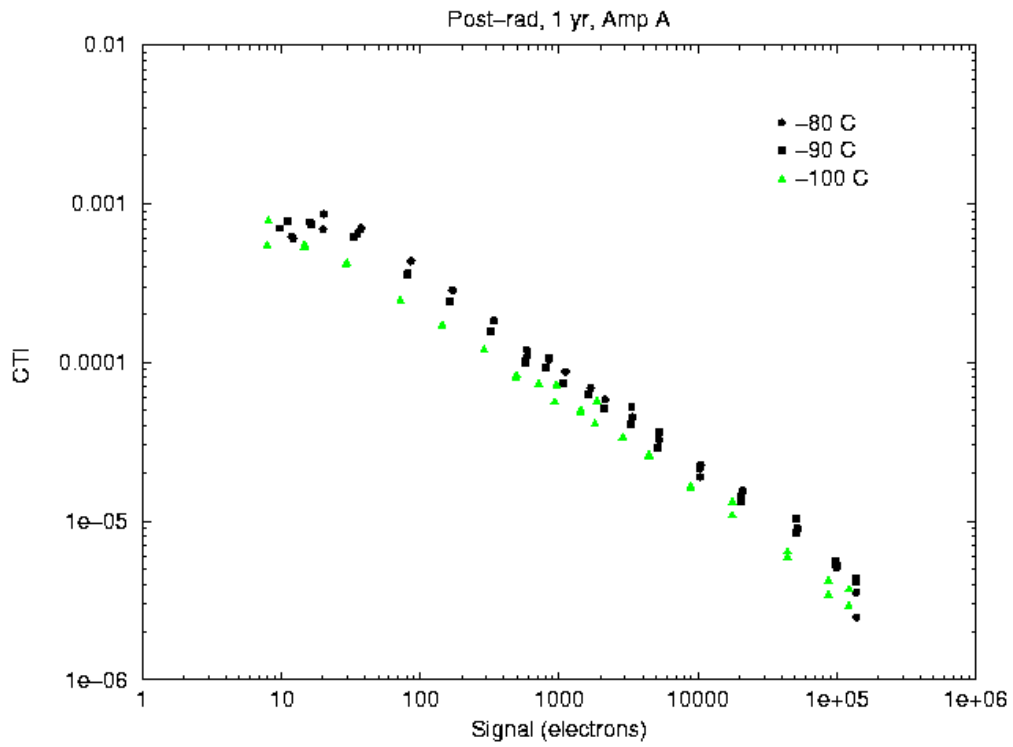


Figure 4a- Parallel CTI FPR Amp A

### CCD44 UV1 Parallel CTI by FPR

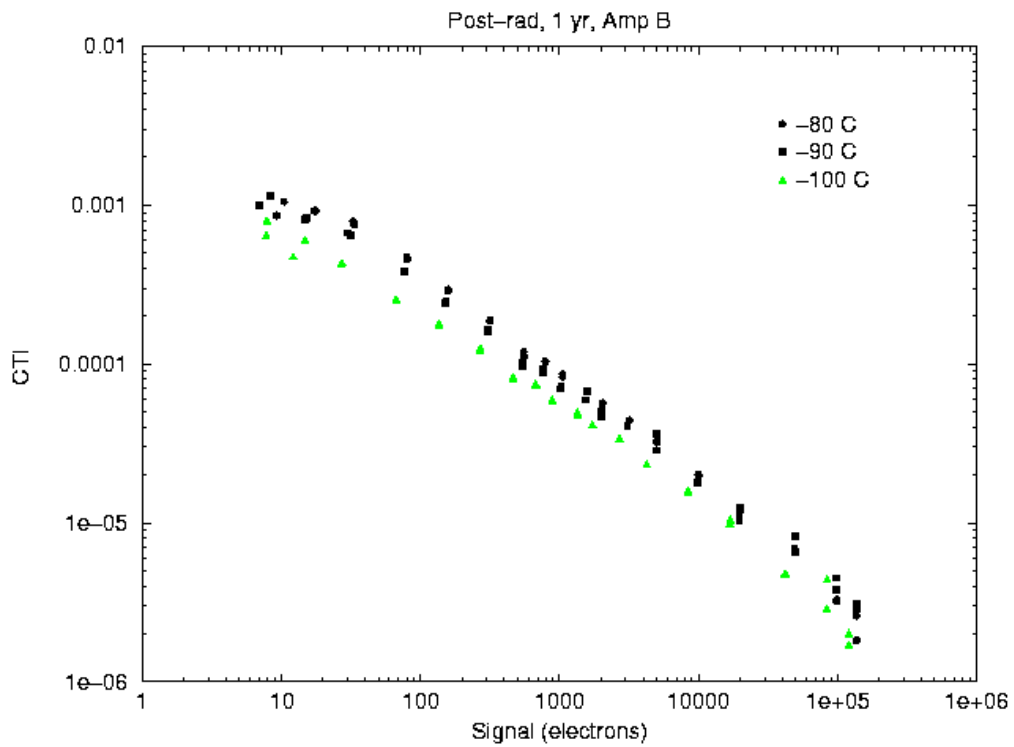


Figure 4b-Parallel CTI FPR Amp B

# CCD44 UV1 Parallel CTI

-90 C, Amp B, Post-rad, 1yr

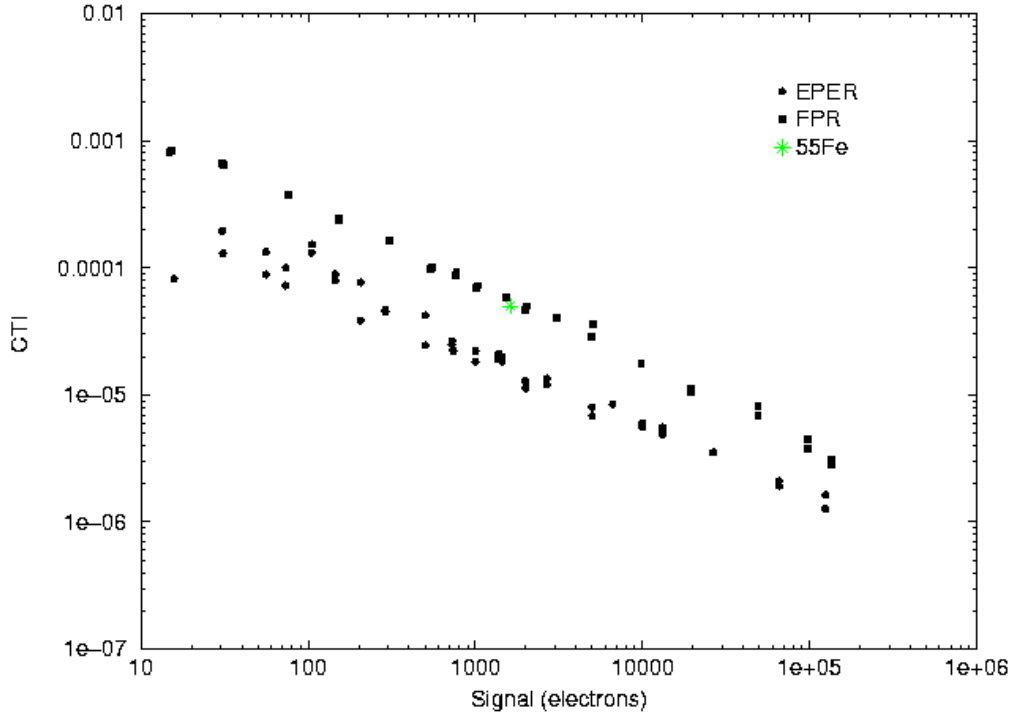


Figure 5-Comparison of Methods

## Acknowledgements:

We gratefully acknowledge the support of Bob Hill, Augustyn Waczynski and Elizabeth Polidan from the Detector Characterization Lab at Goddard Space Flight Center for data acquisition and valuable discussions of analysis techniques and results.